Nuclear Instruments and Methods in Physics Research B 306 (2013) 113–116

Contents lists available at SciVerse ScienceDirect

Nuclear Instruments and Methods in Physics Research B

journal homepage: www.elsevier.com/locate/nimb

Ion-induced fluorescence imaging of endosomes

R. Norarat [a,*], V. Marjomäki [b], X. Chen [c], M. Zhaohong [c], R. Minqin [c], C.-B. Chen [c], A.A. Bettiol [c], H.J. Whitlow [a,1], F. Watt [c]

[a] Department of Physics, University of Jyväskylä, P.O. Box 35 (YFL), FIN-40014 Jyväskylä, Finland
[b] Department of Biological and Environmental Science/Nanoscience Center, University of Jyväskylä, P.O. Box 35 (YFL), FIN-40014 Jyväskylä, Finland
[c] Center for Ion Beam Applications, Department of Physics, National University of Singapore, Science Drive 3, Singapore 117542, Singapore

ARTICLE INFO

Article history:
Received 23 July 2012
Received in revised form 14 December 2012
Accepted 18 December 2012
Available online 18 January 2013

Keywords:
Proton-induced fluorescence (PIF)
Scanning Transmission Ion Microscopy (STIM)
Autofluorescence
Endosomes
Diffraction limit

ABSTRACT

Imaging laboratories at Jyväskylä and Singapore are collaborating on the development of fluorescence imaging of cytoplasmic endosomes using a combination of proton induced fluorescence (PIF) with direct Scanning Transmission Ion Microscopy (direct-STIM) for sub-cellular structural imaging. A549 lung carcinoma cells were cultivated and stained for epidermal growth factor receptor (EGFR) and receptor α2β1 integrin. In this paper, we demonstrate that cells can be imaged at sub-150 nm resolution using the PIF technique. In addition, the same target cell was imaged at 50 and 25 nm resolution by using proton and He-STIM, respectively. The combination of both techniques offer a powerful tool to improve fluorescence imaging beyond optical diffraction limits.

1. Introduction

Enteroviruses are implicated in a range of diseases but the infection mechanism is still poorly understood [1]. Previous studies suggest that Echovirus1 (EV1) infect cells by using multivesicular endosomes (MVBs) [2]. They are difficult to study using fluorescent markers because the virus-containing MVBs are 200 to 500 nm in diameter and at limit of resolution for conventional light microscopy [2–4].

One interesting technique to overcome diffraction limits is proton induced fluorescence (PIF) [5–7]. In previous bio-PIF studies; Pallon et al. [5] measured autofluorescence in cryosectioned skin tissues using panchromatic mapping with a photomultiplier and a spectrophotometer with Si photodiode array for spectral measurements. Rossi et al. [6] took this a step further by using two photomultipliers in coincidence to study common pathological tissue stains of non-fluorescent and fluorescent types. The CIBA group [7] extended this technique to a single cell level achieving ~200 nm resolution for Sytox®green fluorescent stain in N2A blastoma cells by using a highly focused MeV proton beam and collecting the fluorescence signal with a photomulitiplier.

In this paper, we describe development work carried out on A549 lung carcinoma cells, stained for EGFR and receptor α2β1 integrin using proton induced fluorescence (PIF) and both proton and $^4He^+$ direct-Scanning Transmission Ion Microscopy (STIM).

2. Materials and methods

The PIF and high resolution STIM test [8–10] were carried out using the cell imaging facility of the Centre for Ion Beam Applications (CIBA), National University of Singapore, NUS [9]. The A549 lung carcinoma cell samples were prepared at Department of Environmental and Biological Sciences, University of Jyväskylä according to the protocol as described in Table 1. The optical excitation wavelength, emission wavelength and width are, respectively [11]. Alexa 488: 495, 519 and 175 nm. Alexa 555: 555, 565 and 160 nm. The stained cells were checked with an inverted fluorescence microscope (Nikon Eclipse-Ti) [12] to ensure that the vesicles were stained.

A schematic diagram of the PIF technique layout is shown in Fig. 1. The samples were mounted on a target stage, controlled by a stage controller allowing movement in *X*–*Y*–*Z* directions with 25 mm travel. Behind the stage, a Hamamatsu R7400P photomultiplier (PMT) without lens [13] was mounted on a linear positioner to collect the fluorescence signal. The detector which has a wavelength response spanning 160–650 nm was operated in photon counting mode. A 2 MeV proton beam was focused down to sub-150 nm size, and scanned across the target cell on the silicon nitride window as shown in Fig. 1. The PIF images of 512 × 512

* Corresponding author. Tel.: +358 442854705
E-mail address: rattanaporn.norarat@phys.jyu.fi (R. Norarat).
[1] Present address: Institut des Microtechnologies Appliquées Arc, Haute Ecole Arc Ingénierie Eplatures-Grise 17, CH-2300 La Chaux-de-Fonds, Switzerland.

0168-583X/$ - see front matter © 2013 Elsevier B.V. All rights reserved.
http://dx.doi.org/10.1016/j.nimb.2012.12.052

Table 1
Sample preparation protocol.

Culturing of the A549 lung carcinoma cell line: The cells were grown in Dulbecco's modified eagle medium (DMEM) medium at 37 °C in a humidified incubator with 5% CO_2. The silicon nitride window was sterilised with ethanol. After sterilisation, trypsinized cells were plated onto the silicon nitride window in a Petri dish and incubated for 24 h.

Immunofluorescent labelling: The cells were starved for 2 h and then incubated with 1st mouse antibody against integrin at 37 °C for 5 min. The cells were washed three times with PBS, for 5 min each. They were then incubated with 2nd goat-anti-mouse (488 nm) green for 30 min on ice. The cells were again washed three times in PBS. Cells were then stimulated with EGF (100 ng/ml) for 1 h at 37 °C and were subsequently fixed with 4% paraformaldehyde (prepared in PBS, pH 7.4) for 30 min at room temperature. Before immunolabeling, the cells were permeabilized with 0.2% Triton X-100 in PBS for 5 min in room temperature. Subsequently they were incubated with 1st rabbit anti-EGFR (in 3% BSA-PBS) for 1 h. The cells were then washed and incubated with 2nd goat anti-rabbit (555 nm) red for 45 min at room temperature and washed with PBS.

Drying method: The cells were immersed with 50% methanol in water twice for 2 min, then with 100% methanol for 2 min (3×), and then with 50% methanol in tetrabutanol twice for 2 min, following with 100% tetrabutanol for 10 min and hexamethyldisilazane 3 min and then the samples were air-dried.

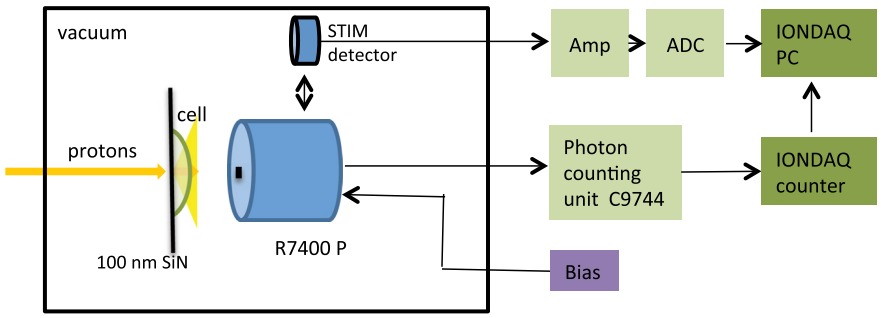

Fig. 1. Schematic diagram of experimental setup. The cell is grown on 100 nm thick silicon membrane. The PMT is placed after the sample with a small piece of Si situated in front of the window to block the proton beam from reaching the PMT. The STIM detector is a PIN diode that is interchanged with the PMT for STIM measurements.

pixels were collected at a count rate of $\sim 1.3 \times 10^4$ counts s^{-1} using IonDaq [14]. Images were taken with 50 μm and 25 μm scan sizes.

The same target cell was also imaged by using the on-axis STIM technique with a spot size 25 and 50 nm for 2 MeV proton and 1.6 MeV $^4He^+$ ions, respectively. This technique is described in Refs. [8–10].

3. Results and discussion

Fig. 2 shows a series of five images of similar cells labelled for α2β1 integrin (green) and EGFR (red). Optical fluorescence images (Fig. 2(a and b)) demonstrate vesicular labelling of integrin and EGFR in separate cytoplasmic vesicles, respectively. A colocalisation can be clearly seen between the PIF image (Fig. 2(c)) and green optical fluorescence image (Fig. 2(a)) and to the lesser degree the PIF-red fluorescence image colocalisation (Fig. 2(b)). It was observed that the detection efficiency of the EGFR signal is very low. Probably this is due to several reasons: (i) The poor quantum detection efficiency of the PMT for red fluorescence (at 600 nm, the response is 15 times lower than 400 nm). (ii) The detection system does not have a narrow bandpass filter which suppresses the autofluorescence [15]. (iii) Spurious fluorescence that may have originated from non-specific binding or sample preparation. This unwanted signal may be stronger than the signal we are interested in, swamping it with unwanted background fluorescence. These effects could be reduced by improved sample preparation and narrow bandwidth filters. In addition, an extended red-response PMT photocathode would enhance detection of the red fluorescence signal.

The correlation between the PIF image (Fig. 3(c)) and the green optical fluorescence image (Fig. 3(a)) is clearly seen. Furthermore in Fig. 3(c) the endosomal vesicles are resolved with finer detail than the green optical fluorescence image seen in Fig. 3(a). Hence, combining structural information from a proton-STIM (Fig. 3(d)) and $^4He^+$-STIM (Fig. 3(e)) technique can help us to understand the multivesicular endosomal structure. In a more general context, the combination of density imaging with direct-STIM and PIF can identify organelles in cells thereby facilitate better interpretation of fluorescence imaging. The image resolutions were estimated from the edge widths in pixels to be 150, 50 and 25 nm fwhm pixel for PIF, $^1H^+$ direct-STIM and $^4He^+$ direct-STIM, respectively.

In confocal-UV fluorescence microscopy studies, colocalization is not observed after internalization in careful confocal quantifications [2] although both kinds of endosomes follow intimately each other. These endosomes share similarities in physical properties accumulating in similar density in sucrose density gradient (data not published), but they still show striking differences in their biochemical properties [2,16]. We have evaluated the colocalization of integrin and EGFR-filled endosomes in other ongoing studies in more detail (Ruusuvuori et al. [17], Quantitative analysis of dynamic association in live biological fluorescent samples, manuscript in revision). The wide-field live data shows 6–16% colocalization after pixel-wise comparison, and the Costes algorithm gives very similar values. These values however, are due to close apposition of the structures and poor resolution, which is apparent in live imaging of these vesicles. And, as said, confocal evaluation of such vesicles give only background values for colocalisation. Therefore, new ways to visualize these multivesicular endosomes with enhanced resolution and the possibility to correlate the data to optical microscopy results is of utmost importance.

There are some questions that need to be resolved however. We do not understand why the endosomes which are stained green appear to be resolved using STIM, whereas the endosomes that are stained red are not. To observe the endosomes using STIM implies that the density of these structures are much higher than the surrounding tissue. Since the protocol for staining was similar in both the red and green cases, the apparent increase in density remains a puzzle.